ISSN 2070-2051, Protection of Metals and Physical Chemistry of Surfaces, 2012, Vol. 48, No. 6, pp. 710–721. © Pleiades Publishing, Ltd., 2012.

INVESTIGATION METHODS FOR PHYSICOCHEMICAL SYSTEMS

Theoretical Study on the Relationship between the Molecular Structure and Corrosion Inhibition Efficiency of Long Alkyl Side Chain Acetamide and Isoxazolidine Derivatives[1]

Yesim S. Kara[a], Seda G. Sagdinc[b], and Asli Esme[c]

[a] *Kocaeli University, Science and Art Faculty, Department of Chemistry, Umuttepe campus, 41380 Kocaeli, Turkey*
[b] *Kocaeli University, Science and Art Faculty, Department of Physics, Umuttepe campus, 41380 Kocaeli, Turkey*
[c] *Kocaeli University, Education Faculty, Umuttepe campus, 41380 Kocaeli, Turkey*
e-mail: seda.sagdinc@gmail.com

Received April 4, 2011

Abstract—Quantum mechanics calculations have been applied to three long alkyl side chain acetamides and three isoxazolidine derivatives used as corrosion inhibitors. The corresponding structures have been optimized, and the highest occupied molecular orbital energy (E_{HOMO}), the lowest unoccupied molecular orbital energy (E_{LUMO}), energy gap (ΔE), electronegativity (χ), hardness (η), softness (σ) and the fraction of electrons transferred from the inhibitor molecule to the metal surface (ΔN) have been calculated using the DFT/B3LYP and HF methods with the 6-31G(d, p) basis set. The electric dipole moment (μ), the mean polarizability ($\langle\alpha\rangle$) and the first order hyperpolarizability (β) values of the investigated molecules have been computed using the same methods. The calculation results also show that the molecules might have microscopic nonlinear optical (NLO) behaviour with non-zero values. Finally, the theoretical results obtained have been compared with the experimental data.

DOI: 10.1134/S2070205112060056

INTRODUCTION

Many organic compounds, particularly long chain fatty acid derivatives, are found to be effective corrosion inhibitors for many metals and alloys. They are substances that minimize or prevent corrosion if corrosion inhibitors are added at low concentrations in an aggressive environment [1]. Two types of adsorption can be envisaged, physical adsorption or chemical adsorption depending on the adsorption strength. The physical adsorption arise from electrostatic interaction between the charged centers of molecules and charged metal surface which results in a dipole interaction of molecules and metal surface, whereas chemical adsorption usually promotes formation of a chelate on the metal surface, which includes the transfer of electrons from the organic compounds to metal, forming coordinate covalent bond [2]. In this way, the metal acts as an electrophile; and the nucleophile centres of the inhibitor molecule are normally heteroatoms with free electron pairs that are readily available for sharing, to form a bond [3].

Cyclic organic compounds with alkyl side chains synthesized as corrosion inhibitors bear two or three of the N, O or S heteroatoms in their constructions. The compounds are adsorbed on the metal surface by these heteroatoms, preventing the destructive effect of such an aggressive acidic medium. Besides these atoms, aromatic ring systems available in the structures of these compounds can also increase adsorptions and consequently enhance the inhibition efficiencies of these compounds with their π electrons [4]. Free electron pairs on heteroatoms or π electrons are readily available for sharing to form a bond and act as the nucleophile centres of inhibitor molecules and greatly facilitate the adsorption process over the metal surface, whose atoms act as electrophiles [5]. The efficiency of an inhibitor does not only depend on its structure, but also on the characteristics of the environment in which it acts and the nature of the metal and other experimental conditions. Under certain conditions, the electronic structure of the organic inhibitors has a key influence on the corrosion inhibition efficiency of the metal [6].

Isoxazolidines, cyclic organic compounds, are efficiently synthesized with 1,3-dipolar cycloaddition which are extensively used in the synthesis of a great many natural products of biological interest [4]. They are also effective corrosion inhibitors due to the presence of adjacent heteroatoms (N–O) with three lone pairs of electrons but there are not many studies about corrosion inhibition efficiencies for isoxazolidines in the literature [1, 7].

Acetamide derivatives have been found by numerous workers to possess sedative, analgesic properties. Many types of derivatives are reported in the literature, especially those having aryl, alkyl and halogen on the

[1] The article is published in the original.

Table 1. Molecular structures, abbreviations and molecular weights of the isoxazolidine and acetamides derivatives

	Compounds used as inhibitors	Abbreviation	Molecular Formula	Molecular Weights
1	5-octylsulfanylmethyl-2,3-diphenyl-isoxazolidine	OSDPI	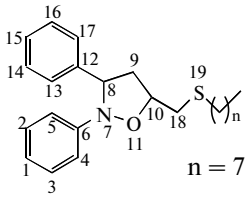 n = 7	383
2	9-(2,3-diphenyl-isoxazolidin-5-yl)-nonanoic acid 2-[2-(2-methoxyethoxy)-ethoxy]-ethyl ester	DPINEE	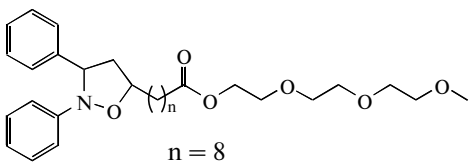 n = 8	527
3	1-(2,3-diphenyl-isoxazolidin-5-yl)-nonan-2ol	DPINO	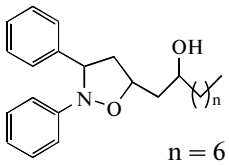 n = 6	367
4	2-(dodecylsulfanyl)-N(pyridin-2yl) acetamide	DSNPA	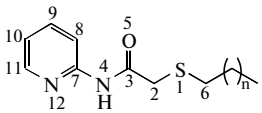 n = 10	336
5	2-(hexadecylsulfanyl)-N-(pyridin-2-yl) acetamide	HSNPA	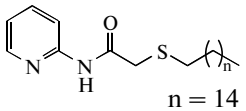 n = 14	392
6	2-(octodecylsufanyl)-N-(pyridin-2-yl) acetamide	OSNPA	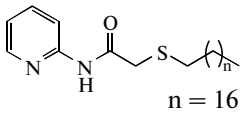 n = 16	420

alpha carbon atom and/or aryl and alkyl groups on the nitrogen of the amide [8]. Amine salts have achieved special importance as corrosion inhibitors for protecting inexpensive materials such as aluminium alloys and low-alloy steels against corrosion in salt and acid solutions [9]. Moreover, nitrogen-containing compounds such as amines and amides have been widely used in oil industries at low temperatures where water phases have been present [10, 11]. The corrosion of iron and steel alloys in contact with oil-in-brine emulsions can be also inhibited in the oil industries by treating the emulsions with oil-soluble, water-soluble or water-dispersible nitrogen-, phosphorus-, and/or sulphur-containing corrosion inhibitors [12].

Recently, 5-octylsulfanylmethyl-2,3-diphenyl-isoxazolidine (OSDPI), 9-(2,3-diphenylisoxazolidin-5-yl)-nonanoic acid 2-[2-(2-methoxy-ethoxy)-ethoxy]-ethyl ester (DPINEE), 1-(2,3)diphenyl-isoxazolidin-5yl)-nonan-2-ol (DPINO) derivatives of isoxazolidine and 2(dodecylsulfanyl)-N-(pyridin-2-yl)acetamide (DSNPA), 2-(hexadecylsulfanyl)-N-(pyridin-2yl)acetamide (HSNPA) and 2-(octadecyl-sulfanyl)-N-(pyridin-2-yl)acetamide (OSNPA) derivatives were synthesized by Yıldırım and Çetin [1], as shown in Table 1. They investigated corrosion inhibitory properties of these compounds in 2 M HCl acidic medium. Sample metals were treated with 50 and 100 ppm concentration for a period of 20 h at room temperature. Inhibition efficiencies were determined by gravimetric method.

Quantum chemical calculations have been used recently to explain the mechanism of corrosion inhibition and proved to be a very powerful tool for studying the mechanism. In our previous study, we investigated whether any clear links exist between the results of quantum chemical calculations and the experimental

corrosion inhibition efficiencies of amides and thiosemicarbazones [13]. One of the aims of this work is to present a theoretical study on the electronic and molecular structural parameters (highest occupied molecular orbital (HOMO) energy, lowest unoccupied molecular orbital (LUMO) energy, the energy gap between E_{HOMO} and E_{LUMO} ($\Delta E = E_{LUMO} - E_{HOMO}$), atomic orbital coefficients and total energies) of some oil-soluble, waterdispersible and N, O and/or S bearing long chain organic compounds, used as inhibitors. In addition, quantum chemical parameters are obtained from the calculations that are responsible for the inhibition efficiency of inhibitors such as electronegativity (χ), hardness (η) and softness (σ) and the fraction of electrons transferred from the inhibitor to iron surface (ΔN).

In recent years, intensive research has addressed the prediction of the nonlinear optical (NLO) properties of organic molecular systems. These molecular systems are attracting a great deal of attention, as they have large optical susceptibilities, inherent ultrafast response times and high optical thresholds for laser power as compared with inorganic materials [14]. Polarizability (α) and hyperpolarizability (β) properties of organic material is used in searching for suitable materials for optoelectronic devices. These are obtained as the first and second derivatives of the induced dipole moment with respect to the applied field, respectively. The polarizabilities are all second derivatives of the electronic energy with respect to field components, field gradient components, so on. The organic systems having a hyperpolarizability coefficient β greater than zero are well suited for use in the field nonlinear optics. Also, in previous studies [3, 5, 13] are shown that polarizability is one of the main factors in electrostatic interaction between an inhibitor molecule and a metal. Therefore, another aims of this work are to report the results of the calculation of the dipole moment (μ), the mean polarizability ($\langle\alpha\rangle$) and the first order hyperpolarizability (β) of isoxazolidine and acetamide molecules and to investigate the relationship between these parameters and inhibition efficiencies, by using the DFT and HF methods [4].

METHODS

The geometry pre-optimizations of the molecules studied have been carried out by applying the molecular-mechanics method with the MM+ force field using the HyperChem-7.5 software [15]. Thereafter, the optimized equilibrium structures of molecules have been calculated at the B3LYP and HF methods' 6-31G(d, p) basis set using the GaussView visualization program [16] and the Gaussian 03 program package [17].

The density functional theory (DFT) has been found to be successful in providing insights into chemical reactivity and selectivity, in terms of global parameters such as chemical potential (μ), electronegativity (χ), hardness (η) and softness (σ) [18]. For an N-electron system with total electronic energy (E) and an external potential $v(\vec{r})$ that the electrons feel due to the nuclei, the chemical potential (μ) known as the negative of electronegativity (χ) has been defined as the first derivative of the E with respect to N at

$$\mu = -\chi = \left(\frac{\partial E}{\partial N}\right)_{v(\vec{r})}.$$

Hardness (η) has been defined within the DFT as the second derivative of the E with respect to N at

$$\eta = \frac{1}{2}\left(\frac{\partial^2 E}{\partial N^2}\right)_{v(\vec{r})}.$$

Two systems, Fe and inhibitor, are brought together; electrons flow from the lower χ (inhibitor) to the higher χ (Fe), until the chemical potentials become equal. As a first approximation, the fraction of electrons transferred, ΔN is given by [19]

$$\Delta N = \frac{\chi_{Fe} - \chi_{inh}}{2(\eta_{Fe} + \eta_{inh})},$$

where Fe is the Lewis acid according to the HSAB theory [20]. The difference in electronegativity drives the electron transfer, and the sum of the hardness parameters acts as a resistant [19].

In a finite difference approximation, with the assumption that the energy varies quadratically with the number of electrons, these two quantities for the inhibitor molecule can be expressed with an orbital basis set as follows [21]:

$$\chi = (I + A)/2, \quad \eta = (I - A)/2,$$

where I is the ionization potential and A is the electron affinity of a system.

According to Koopman's theorem [22], the energies of the HOMO and the LUMO of the inhibitor molecule are related to the ionization potential and the electron affinity respectively by the following relations:

$$I = -E_{HOMO}, \quad A = -E_{LUMO}.$$

The softness σ of the inhibitor molecule is simply the inverse of the hardness [23]:

$$\sigma = 1/\eta.$$

In this paper, we are presenting values of the mean polarizability (α) as defined in the following equation:

$$\langle\alpha\rangle = \frac{1}{3}(\alpha_{xx} + \alpha_{yy} + \alpha_{zz})$$

and sometimes the anisotropy ($\Delta\alpha$), which is written here in an obvious notation as [24]:

$$\Delta\alpha = \left\{\frac{(\alpha_{xx} - \alpha_{yy})^2 + (\alpha_{xx} - \alpha_{zz})^2 + (\alpha_{zz} - \alpha_{yy})^2 + 6(\alpha_{xy}^2 + \alpha_{xz}^2 + \alpha_{yz}^2)}{2}\right\}^{1/2}.$$

Table 2. Calculated energy (eV) levels of the E_{HOMO}, E_{LUMO}, ($\Delta E = E_{LUMO} - E_{HOMO}$), total energies and the measured average inhibition efficiencies (%) at 50 and 100 ppm concentration of 2 M HCl solution [1] for the series of studied molecules

Molecules		OSDPI	DPINEE	DPINO	DSNPA	HSNPA	OSNPA
B3LYP 6-31G(d.p)	E_{HOMO}	−5.064	−5.264	−5.172	−5.931	−5.931	−5.931
	E_{LUMO}	−0.094	−0.194	−0.367	−0.736	−0.736	−0.736
	ΔE	4.970	5.070	4.806	5.194	5.194	5.194
	Total Energy	−39799.3	−46653.4	−31010.9	−36090.6	−40370.01	−42509.72
HF 6-31G(d.p)	E_{HOMO}	−7.717	−8.034	−7.800	−8.692	−8.691	−8.691
	E_{LUMO}	3.802	3.727	3.643	3.368	3.369	3.369
	ΔE	11.520	11.761	11.443	12.060	12.060	12.056
	Total Energy	−38526.96	−46361.17	−30809.42	−34843.05	−40154.39	−42278.94
Inhibition eff. % (IE %) [1]	50 ppm	91	88.6	83.9	91.2	90.9	84.1
	100 ppm	88.3	86	80.9	82.2	80.6	58.3

The first hyperpolarizability (β) reported here is defined as [25]

$$\beta_{total} = [(\beta_{xxx} + \beta_{xyy} + \beta_{xzz})^2 + (\beta_{yyy} + \beta_{yzz} + \beta_{yxx})^2 + (\beta_{zzz} + \beta_{zxx} + \beta_{zyy})^2]^{1/2}.$$

The α and β components of the GAUSSIAN 03W output are reported in atomic units, thus the calculated values have to be converted into electrostatic units (α: 1 a.u.= 0.1482×10^{-24} esu; β: 1 a.u. = 8.6393×10^{-33} esu) [26].

RESULTS AND DISCUSSION

The molecular structures of isoxazolidine [5-octylsulfanylmethyl-2,3-diphenyl-isoxazolidine (OSDPI), 9-(2,3-diphenyl-isoxazolidin-5-yl)-nonanoic acid 2-[2-(2-methoxy-ethoxy)ethoxy]-ethyl ester (DPINEE), 1-(2,3-diphenyl-isoxazolidin-5-yl)-nonan-2-ol (DPINO)], 2(dodecylsulfanyl)-N-(pyridin-2-yl)acetamide (DSNPA), 2-(hexadecylsulfanyl)-N-(pyridin-2yl)acetamide (HSNPA) and 2-(octodecylsulfanyl)-N-(pyridin-2-yl)acetamide (OSNPA) calculated by the B3LYP/6-31G(d,p) level are shown in Fig.1, respectively.

The ground state geometry of the inhibitor as well as the nature of its frontier molecular orbitals, namely the HOMO and LUMO, is involved in the activity properties of the inhibitors. The HOMO and LUMO electron densities calculated by the B3LYP method using the 6-311G(d,p) basis set of molecules studied in the ground state are also shown in Fig. 1.

E_{HOMO} is often associated with the electron-donating ability of a molecule, whereas E_{LUMO} indicates its ability to accept electrons [27]. The gap energy, $\Delta E = (E_{LUMO} - E_{HOMO})$, is an important parameter as a function of the reactivity of the inhibitor molecule towards the adsorption on the metallic surface. Quantum chemical indices are obtained from the calculations such as E_{HOMO}, E_{LUMO} and $\Delta E = E_{LUMO} - E_{HOMO}$ and the total energies are summarized in Table 2. The measured average inhibition efficiencies (%) of these molecules are also listed in the table (these data have been measured in 2 M HCl for 20 h at room temperature for 50 and 100 ppm inhibitor concentrations). Yıldırım and Çetin [1] found approximately equal (except 100 ppm concentration for OSNPA) inhibiting effectiveness. This same trend reflects the important role played by the molecular size and the substituent groups of the inhibitor molecule as well as the types of functional group adsorption atom in the inhibition process [3]. Many researchers have reported that the inhibiting effect of the compounds can be ascribed to their parallel adsorption at the metal solution interface. The parallel adsorption is attributed to the presence of one or more active centres for adsorption [28, 29]. According to Yıldırım and Çetin' s study [1], most of the investigated acetamide and isoxazolidine derivatives containing sulphur atoms in their long alkyl side chains showed a promising protection of metal. This was an expected result due to the high electron releasing effect of sulphur atoms. As is known, besides being structures of these heteroatoms, π electrons available in the various functional groups can also facilitate adsorption of corrosion inhibitors to the metal surface and increase their inhibition efficiencies [30]. The isoxazolidine derivatives contain two benzene rings, in other words a π electron system. Having the two benzene rings, which makes its dispersion easy in an acidic aqueous medium, improves the inhibitory properties of the isoxazolidine derivatives. DPINO molecules possess polar-OH functional groups on their C atoms vicinal to the heterocyclic part. Thus they exhibit excellent corrosion inhibition. Polar ester groups present in the structures of

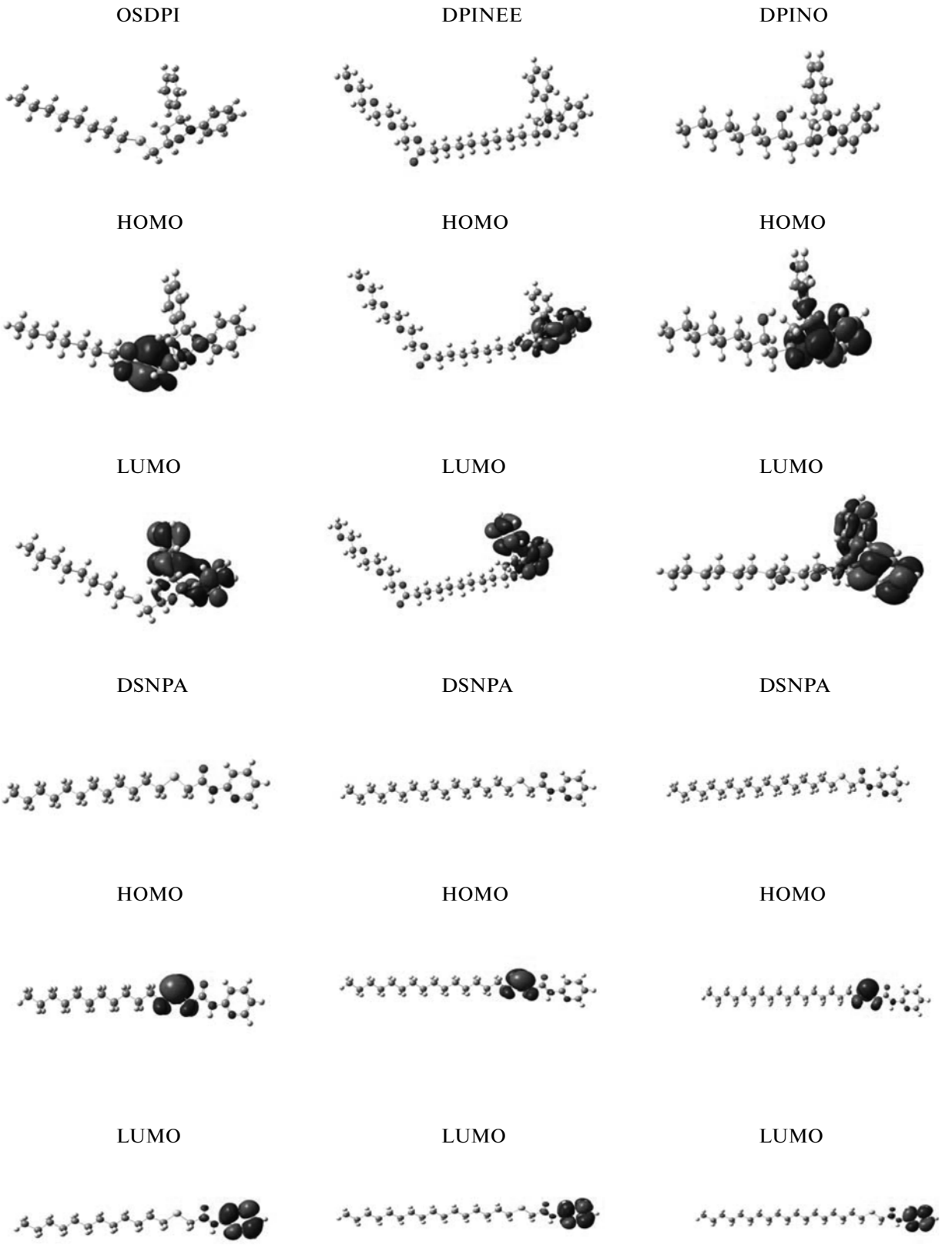

Fig. 1. Molecular structures and HOMO-LUMO of 5-octylsulfanylmethyl-2,3diphenyli soxazolidine (**OSDPI**), 9-(2,3-diphenyl-isoxazolidin-5-yl)-nonanoic acid 2-[2-(2-methoxy-ethoxy)-ethoxy]-ethyl ester (**DPINEE**), 1-(2,3-diphenylisoxazolidin-5-yl)-nonan-2-ol (**DPINO**), 2-(dodecylsulfanyl)-N-(pyridin-2yl) acetamide (**DSNPA**), 2-(hexadecylsulfanyl)-N-(pyridin-2yl) acetamide (**HSNPA**), 2(octodecylsulfanyl)-N-(pyridin-2yl) acetamide (**OSNPA**), derivatives.

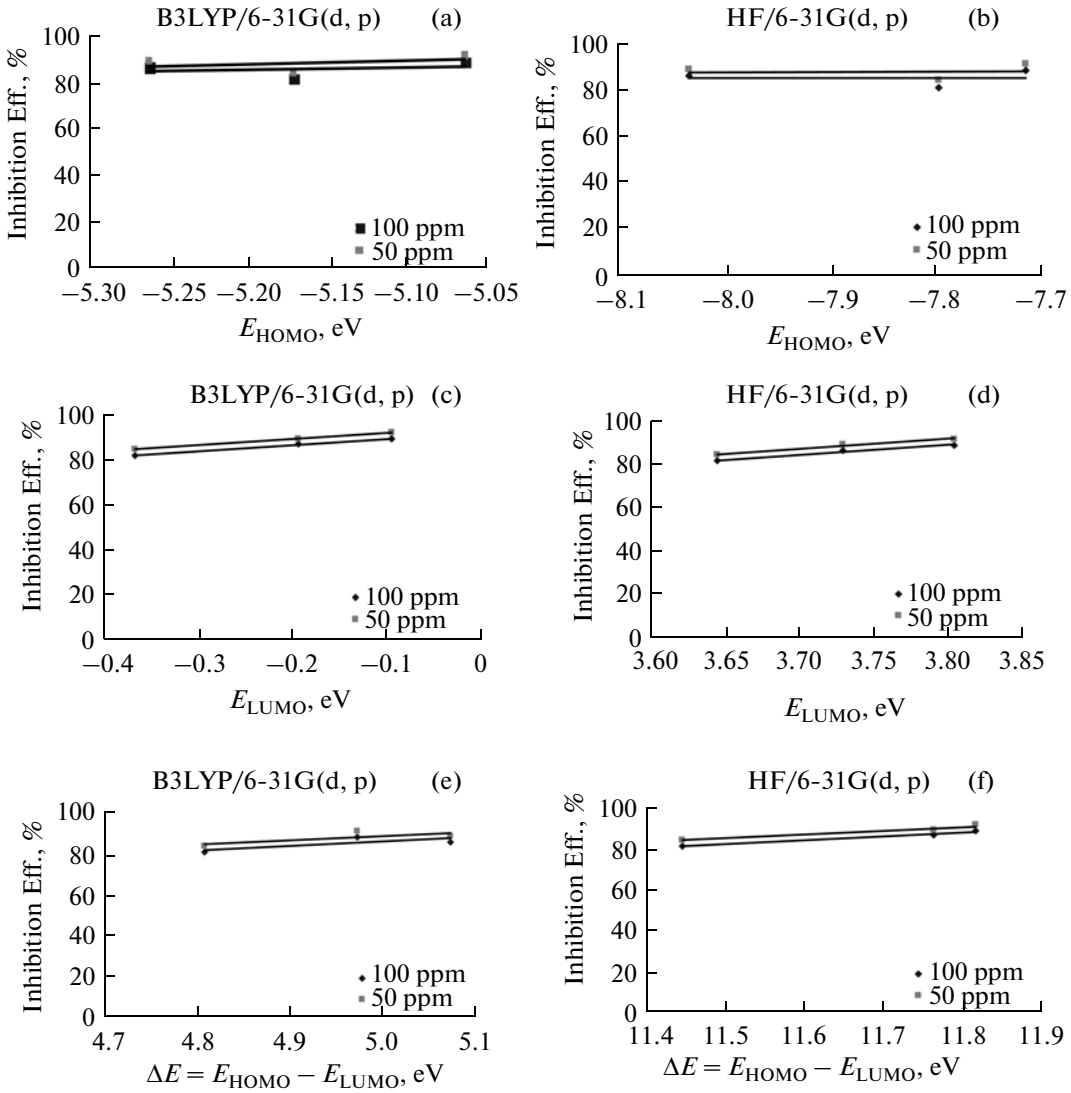

Fig. 2. Plots of E_{HOMO}, E_{LUMO}, and $\Delta E = E_{HOMO} - E_{LUMO}$ (eV) energy gap versus % corrosion inhibition efficiencies of isoxazolidine derivatives used.

DPINEE enhance its dispersing properties in water. Consequently, the ester functional group of DPINEE forces the inhibitor molecules into an approximately perpendicular orientation at the metal surface [1].

We have not been able to find a direct relationship between all the inhibition efficiencies and energy levels. The relationships between the corrosion inhibition efficiencies of isoxazolidine derivatives and E_{HOMO}, E_{LUMO} and $\Delta E = (E_{LUMO} - E_{HOMO})$ are plotted in Fig. 2. As seen in Fig. 2, no direct correlations between the inhibition efficiencies and the E_{HOMO}, E_{LUMO} and $\Delta E = (E_{LUMO} - E_{HOMO})$ obtained using B3LYP/6-31G(d, p) and HF/6-31G(d, p) for isoxazolidine and acetamide derivatives could be found. It is attributed to the long alkyl (CH_2) chains of acetamide derivatives. This result was explained by Ali and co-workers as being due to the fact that inhibition increases with the carbon number in the chain to about 10 carbons, but with higher members little increase or decrease in the ability to inhibit corrosion occurs [31].

The total energy calculated by quantum chemical methods is also a beneficial parameter. The total energy of a system is composed of the internal, potential and kinetic energy. Hohenberg and Kohn [32] proved that the total energy of a system, including that of the many body effects of electrons (exchange and correlation) in the presence of the static external potential (for example, the atomic nuclei), is a unique functional of the charge density. The minimum value of the total energy functional is the ground state energy of the system. As seen in Table 2, the lower total energy obtained for acetamide derivative is related to OSNPA, which exhibits weaker inhibition. The higher total energy (–34843.05 eV) confirms the higher stability of DSNPA. The reason is that acetamide derivatives are different from each other only CH_2 group

Table 3. Electronegativity (χ), hardness (η), softness (σ), the fraction of electron transferred Δ*N* for molecules with inhibitor properties studied

Molecules	χ, eV		η, eV		σ, 1/eV		Δ*N*	
	B3LYP 6-31G(d, p)	HF 6-31G(d, p)	B3LYP 6-31G(d, p)	HF 6-31G(d, p)	B3LYP 6-31G(d, p)	HF 6-31G(d, p)	B3LYP 6-31G(d, p)	HF 6-31G(d, p)
OSDPI	2.580	1.958	2.485	5.760	0.402	0.174	0.889	0.438
DPINEE	2.729	2.153	2.535	5.880	0.394	0.170	0.843	0.412
DPINO	2.770	2.079	2.403	5.721	0.416	0.175	0.880	0.430
DSNPA	3.335	2.662	2.597	6.030	0.385	0.166	0.706	0.360
HSNPA	3.333	2.662	2.597	6.030	0.385	0.166	0.706	0.360
OSNPA	3.333	2.661	2.597	6.030	0.385	0.166	0.706	0.360

Note: Using DFT and HF methods with 6-31G(d, p) basis set in the present work.

number at tail of molecules. Also, no correlation is found to exist between the total energy and the corrosion inhibition values of isoxazolidine derivatives since their tails are completely different.

In Table 3 the results for the calculations of the electronegativity (χ), hardness (η), softness (σ) and the fraction of electron transferred Δ*N* for the derivatives studied are presented. In the reactions of the two systems with different electronegativities (as a metallic surface and an inhibitor molecule) the following mechanism takes place [33]: the electron flow happens from the molecule with the low electronegativity towards that with a higher value, until the chemical potentials are the same. In our calculation using the B3LYP and HF methods with the 6-31G(d, p) basis set, the best inhibitory effect is found by OSDPI for isoxazolidine derivatives with low electronegativity (2.580 eV for the B3LYP/6-31G(d,p) method and 1.958 eV for the HF/6-31G(d, p) method). Besides, DPINO exhibits the lowest value of hardness. It is means that the latter has the higher reactivity, and then OSDPI and DPINEE. In the literature it has been reported that the values of Δ*N* show that the inhibition effect results from electrons donation [33, 34]. According to Lukovits's study [34], if the value of Δ*N*, the inhibition efficiency increases with the increasing electron donating ability of the inhibitor at Δ*N*. Furthermore, it has been observed [35] that inhibition efficiency increases with an increase in the values of Δ*N*. However, our study reveals that there is no regular trend in the inhibition efficiency by increasing values of Δ*N*.

The dipole moment (μ) is an index that can also be used for the prediction of the direction of a corrosion inhibition process. The dipole moment is the measure of polarity in a bond and is related to the distribution of electrons in a molecule [36]. Although the literature is inconsistent over the use of μ as a predictor for the direction of a corrosion inhibition reaction, it is generally agreed that the adsorption of polar compounds possessing high dipole moments on the metal surface should lead to better inhibition efficiency. A comparison of the results obtained from the dipole moment with experimental inhibition efficiencies indicate that the % inhibition efficiencies of the inhibitors increase with an increase in the value of the dipole moment for isoxazolidine derivatives (Fig. 3). The relationship between the inhibition efficiencies of these molecules and the dipole moment obtained using B3LYP/6-31G(d, p) and HF/6-31G(d, p) for isoxazolidine derivatives are 99.95 and 89.32% for a 50 ppm inhibitor concentration and 96.37 and 87.92% for a 100 ppm inhibitor concentration, respectively.

Polarizability and hyperpolarizability characterize the response of a system in an applied electric field [37]. This means polarizability is also the ratio of the

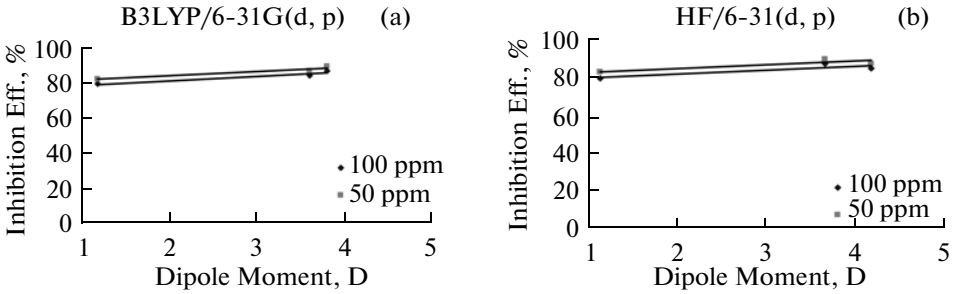

Fig. 3. Plots of dipole moments versus % corrosion inhibition efficiency of isoxazolidine derivatives used.

Table 4. The mean ($\langle\alpha\rangle$) polarizabilities, the anisotropy polarizabilities ($\langle\Delta\alpha\rangle$), the electric dipol moments (μ), the first-order hyperpolarizabilities (β_{tot}) and the measured average inhibition efficiencies [1] of the studied molecules from DFT and HF calculations

B3LYP/6-31G(d, p) [HF/6-31G(d, p)]	OSDPI	DPINEE	DPINO	DSNPA	HSNPA	OSNPA
$\langle\alpha\rangle \times 10^{-24}$ esu	23.53	34.65	23.83	144.28	171.17	184.64
	(23.68)	(34.74)	(24.03)	(146.64)	(174.14)	(187.92)
$\langle\Delta\alpha\rangle$ au.	14.85	61.31	21.25	27.01	34.06	38.53
	(15.44)	(59.12)	(20.59)	(28.11)	(35.72)	(40.58)
$\beta_{tot} \times 10^{-30}$ esu	0.24	4.83	0.59	3.65	5.34	6.21
	(0.33)	(5.24)	(0.79)	(3.96)	(5.71)	(6.61)
β_{tot}/β_{urea}	1.2	24.81	3.03	18.75	27.42	31.91
	(1.7)	(26.91)	(4.06)	(20.34)	(29.33)	(33.94)
Dipole moment (D)	3.80	3.60	1.1796	2.852	2.852	2.853
	(3.63)	(4.14)	(1.11)	(3.11)	(3.10)	(3.10)
Inhib. eff. % 50 ppm	91	88.6	83.9	91.2	90.9	84.1
(IE%)[1] 100 ppm	88.3	86	80.9	82.2	80.6	58.3

induced dipole moment to the intensity of the electric field, that is, the induced dipole moment is proportional to polarizability, which increases with the increase in the molecular volume [38]. The dipole hyperpolarizability is obtained as the second derivative of the energy. They determine not only the strength of molecular interactions (such as the long-range intermolecular induction, dispersion forces, etc.) as well as the cross sections of different scattering and collision processes, but also the nonlinear optical properties of the system [39–42]. Here we have computed the polarizability and the first hyperpolarizabilities as a numerical derivative of the dipole moment using the B3LYP/6-31G(d, p) and HF/6-31G(d, p) methods.

In Table 4, the calculated mean polarizability ($\langle\alpha\rangle$), anisotropy ($\Delta\alpha$) and first hyperpolarizability (β) values for the studied molecules are calculated and reported. The HF values are presented in brackets. The results do not show very distinct polarizabilities at the HF and B3LYP levels. As seen from Table 4, the first hyperpolarizabilities of the molecules studied are predicted for the first time in this new class of compounds, and calculated to be between 0.24×10^{-30} esu (for OSDPI using B3LYP) and 6.61×10^{-30} esu (for OSNPA using HF). Since there are not any reported experimental values for the first hyperpolarizability of the title compounds in the literature, the experimental values of urea ($\beta = 0.1947 \times 10^{-30}$ esu) have been used for a comparison (β_{tot}/β_{urea}). The title compounds are good candidates as second-order nonlinear optical materials because their first hyperpolarizabilities have been changed between 1.2 and 31.92 times that of urea. Moreover, the magnitudes of β for acetamide derivatives increase while the corrosion inhibition values decrease (Table 4).

Mulliken population analysis [43] is mostly used for the calculation of the charge distribution in a molecule. These numerical quantities are easy to obtain and they provide at least a qualitative understanding of the structure and reactivity of molecules. The atomic charges of the studied molecules obtained by Mulliken's population analysis are shown in Table 5. These charges indicate that there is more than one active centre and it is confirmed that the more negative the atomic partial charges of the adsorbed centre is, the more easily the atoms donate its electrons to the unoccupied d-orbital of the metal [44–46]. It is found that high negative charges are N4, O5 and N12 atoms for acetamides. Hence these atoms are the most probable centre of adsorption via the lone pair electrons in acetamide derivatives. S1 has positive charge [0.147e for B3LYP/6-31G(d, p), 0.205e for HF/6-31G(d, p)] for these molecules, while O5 atom has negative charge due to polarizability of C=O group. Therefore, the O5 atom in the C=O group is the probable centre of adsorption via the lone pair electrons in the acetamide derivatives.

The calculation shows that N7, O11 and C18 are high negative charges for isoxazolidine derivatives. Hence these atoms are the most probable centres of adsorption via the lone pair electrons in isoxazolidine derivatives. A positive charge of S19 is found in OSDPI [0.099e for B3LYP/6-31G(d, p), 0.135e for HF/6-31G(d, p)].

Tables 6 and 7 give the coefficients of the atoms of the HOMO and LUMO calculated using the B3LYP/6-31G(d, p) of the molecules studied. The standard 6-31G(d, p) basis set is a split valence basis set 6-31G [47–51], with added single first polarization functions, one set of d functions on the heavy atoms and one set of p functions on the hydrogens [52]. Only atomic orbitals of the valance for isoxazolidine derivatives take part: $2p_x$, $2p_y$, $2p_z$, 3s, $3p_x$, $3p_z$ for C, N, O and S atoms. The S atom is found to have the highest

Table 5. Charges of C, N, O, S atoms for studied molecules by using B3LYP/6-31G(d, p) and HF/6-31G(d, p) methods

Atoms	B3LYP/6-31G(d, p)			HF/6-31G(d, p)			Atoms	B3LYP/6-31G(d, p)			HF/6-31G(d, p)		
	OSDPI	DPINEE	DPINO	OSDPI	DPINEE	DPINO		DSNPA	HSNPA	OSNPA	DSNPA	HSNPA	OSNPA
C1	–0.089	–0.085	–0.089	–0.170	–0.161	–0.172	S1	0.147	0.147	0.147	0.205	0.205	0.205
C2	–0.097	–0.104	–0.094	–0.137	–0.148	–0.137	C2	–0.433	–0.433	–0.433	–0.489	–0.489	–0.489
C3	–0.095	–0.097	–0.097	–0.138	–0.146	–0.135	C3	0.599	0.599	0.599	0.768	0.768	0.768
C4	–0.109	–0.093	–0.109	–0.170	–0.138	–0.174	N4	–0.590	–0.590	–0.590	–0.794	–0.794	–0.794
C5	–0.102	–0.109	–0.112	–0.163	–0.173	–0.174	O5	–0.475	–0.475	–0.475	–0.575	–0.575	–0.575
C6	0.292	0.280	0.287	0.293	0.284	0.291	C6	–0.433	–0.336	–0.335	–0.387	–0.387	–0.387
N7	–0.308	–0.320	–0.301	–0.381	–0.390	–0.376	C7	0.466	0.467	0.467	0.588	0.588	0.588
C8	0.020	–0.419	–0.429	0.094	0.105	0.097	C8	–0.089	–0.089	–0.089	–0.202	–0.202	–0.202
C9	–0.244	–0.238	–0.251	0.289	0.135	–0.294	C9	–0.070	–0.070	–0.070	–0.089	–0.089	–0.089
C10	0.237	0.200	0.219	0.269	0.252	0.254	C10	–0.101	–0.101	–0.101	–0.223	–0.223	–0.223
O11	–0.409	–0.419	–0.429	–0.524	–0.540	–0.543	C11	0.100	0.100	0.100	0.143	0.143	0.143
C12	0.123	0.093	0.132	–0.020	–0.042	–0.014	N12	–0.519	–0.519	–0.519	–0.628	–0.628	–0.628
C13	–0.130	–0.121	–0.122	–0.163	–0.157	–0.157	–	–	–	–	–	–	–
C14	–0.086	–0.088	–0.083	–0.136	–0.145	–0.140	–	–	–	–	–	–	–
C15	–0.085	–0.084	–0.083	–0.149	–0.153	–0.153	–	–	–	–	–	–	–
C16	–0.085	–0.087	–0.082	–0.146	–0.145	–0.144	–	–	–	–	–	–	–
C17	–0.088	–0.108	–0.169	–0.151	–0.137	–0.188	–	–	–	–	–	–	–
C18	–0.377	–0.182	–0.206	–0.412	–0.219	–0.237	–	–	–	–	–	–	–
S19	0.099	–	–	0.135	–	–	–	–	–	–	–	–	–
O21	–	–	–0.554	–	–	–0.666	–	–	–	–	–	–	–

Table 6. AO coefficients of HOMO for studied molecules by using B3LYP/6-31G(d, p)

No	AO	OSDPI	DPINEE	DPINO	No	AO	DSNPA	HSNPA	OSNPA
C1	$2p_x$	–	0.16221	0.13860	S1	$2p_z$	–0.24845	–0.24845	–0.24844
	$2p_y$	–	–0.15376	–0.14279		$3p_z$	0.65787	0.65786	0.65784
	$2p_z$	–	–	0.13804		$4p_z$	0.40354	0.40354	0.40353
	$3p_x$	–	0.12970	0.11520	C3	$2p_z$	–	–	–
	$3p_y$	–	–0.12434	0.11154		$3p_z$	–	–	–
	$3p_z$	–	–	0.11025	N4	$2p_z$	0.11838	0.11838	0.11842
C2	$3p_y$	–	–	–		$3p_z$	0.10015	0.10015	0.10018
C3	$3p_x$	–	–	–	O5	$2p_z$	–	–	–
	$3p_y$	–	–	–		$3p_z$	–	–	–
	$3p_z$	–	–	–	C7	$2p_z$	–	–	–
C4	$2p_y$	0.13192	–0.19267	0.10987		$3p_z$	–	–	–
	$2p_z$	–	–	–0.10449	C8	$3p_z$	–	–	–
	3s	–	0.19228	–0.11759	C9	$2p_z$	–	–	–
	$3p_x$	–	0.13626	–0.10191		$3p_z$	–	–	–
	$3p_y$	0.12689	–	–	C10	$2p_z$	–	–	–
	$3p_z$		–0.13409	–		$3p_z$	–	–	–
					C11	$2p_z$	–	–	–
C5	$2p_x$	–0.10180	–0.19459	–0.11759		$3p_z$	–	–	–
	$2p_y$	0.13599	0.19633	0.10987	N12	$2p_z$	–	–	–
	$2p_z$		–	–0.10315		$3p_z$	–	–	–
	$3p_x$	–0.10168	–0.13306	–			–	–	–
	$3p_y$	0.11463	0.14051	–					
	$3p_z$	–	–	–0.10545					
C6	$2p_x$	–0.11585	–0.15041	–					
	$2p_y$	0.16861	–	–					
	$2p_z$	–0.12518	–	–0.12312					
	$3p_x$	–0.12004	–	–					
	$3p_y$	0.13156	0.10920	0.17787					
N7	$2p_x$	0.13666	0.35860	–					
	$2p_y$	–0.19655	–0.15878	–0.22588					
	$2p_z$	0.20258	–	0.28157					
	3s	0.13797	–0.18699	0.17066					
	$3p_x$	0.11797	0.29188	0.14999					
	$3p_y$	–0.18281	–0.12494	–0.17000					
	$3p_z$	0.19410	–	0.22418					
C8	3s	–	0.13030	–0.10587					
	$3p_y$	–	–	–					
C9	3s	–	–	–					
	$3p_z$	–	–	–					
C10	3s	–	–	–					
O11	$2p_x$	–0.16421	–0.22788	–0.15424					
	$2p_y$	0.14346	0.15065	0.18106					
	$2p_z$	–0.12447	–0.11458	–0.11185					
	$3p_x$	–0.12906	–0.19268	–0.12083					
	$3p_y$	0.11310	0.10530	0.14282					
	$3p_z$	–	–	–0.09013					
C13	3s	–	0.10341	–					
C14	$2p_x$	–	–	–					
	$2p_y$	–	–	–					
	$3p_x$	–	–	–					
	$3p_y$	–	–	–					
	$3p_z$	–	–	–					
C15	$2p_x$	–	–	–					
	$2p_y$	–	–	–					
	$2p_z$	–	–	–					
	$3p_x$	–	–	–					
	$3p_z$	–	–	–					
C16	$2p_x$	–	–	–					
	$3p_x$	–	–	–					
S20	$2p_y$	–0.22378	–	–					
	$3p_x$	0.21966	–	–					
	$3p_z$	0.23612	–	–					

Table 7. AO coefficients of LUMO for studied molecules by using B3LYP/6-31G(d, p)

No	AO	OSDPI	DPINEE	DPINO	No	AO	DSNPA	HSNPA	OSNPA
C1	$2p_x$	–	–	–	S1	$2p_z$	–	–	–
	$2p_y$	–	–	–		$3p_z$	–	–	–
	$2p_z$	–	–	–		$4p_z$	–	–	–
	$3p_x$	–	–	–	C2	$2p_z$	–	–	–
	$3p_y$	–	–	–		$3p_z$	–	–	–
	$3p_z$	–	–	–	C3	$2p_Z$	0.24476	0.24472	0.24469
C2	$3p_y$	0.12454	–	–		$3p_Z$	0.19515	0.19512	0.19509
C3	$3p_x$	0.16894	–	–	N4	$2p_z$	–	–	–
	$3p_y$	–	–	–		$3p_z$	–	–	–
		0.19247							
	$3p_z$	0.11463	–	–	O5	$2p_z$	−1.17555	−0.17553	−0.17551
C4	$2p_y$	–	–	–		$3p_z$	−0.18030	−0.18027	−0.18025
	$2p_z$	–	–	–	C7	$2p_z$	−0.27195	−0.27195	−0.27194
	3s	–	–	–		$3p_z$	−0.27895	−0.27895	−0.27894
	$3p_x$	0.11629	–	–	C8	$3p_z$	−0.11528	−0.11528	−0.11530
	$3p_y$	–	–	–	C9	$2p_z$	0.33099	0.33099	0.33100
		0.17090							
	$3p_z$	0.14728	–	–		$3p_z$	0.41897	0.41897	0.41899
C5	$2p_x$	–	–	–	C10	$2p_z$	−0.20097	−0.20094	−0.20093
	$2p_y$	–	–	–	C11	$3p_z$	−0.26681	−0.26677	−0.26676
	$2p_z$	–	–	–		$2p_z$	−0.13308	−0.13313	−0.13316
	$3p_x$	–	–	–		$3p_z$	−0.14086	−0.14092	−0.14095
	$3p_y$	–	–	–	N12	$2p_z$	0.33491	0.33492	0.33493
	$3p_z$	–	–	–		$3p_z$	0.37099	0.37101	0.37102
C6	$2p_x$	–	–	–					
	$2p_y$	–	–	–					
	$2p_z$	–	–	–					
	$3p_x$	–	–	–					
	$3p_y$	–	–	–					
N7	$2p_x$	–	–	0.10785					
	$2p_y$	–	–	–					
	$2p_z$	–	–	–					
	3s	–	–	–					
	$3p_x$	–	–	–					
	$3p_y$	–	–	–					
	$3p_z$	–	0.10247	–					
C8	3s	–	–	–					
	$3p_x$	–	–	–					
	$3p_y$	–	−0.13180	−0.13180					
C9	3s	–	–	−0.22471					
	$3p_x$	–							
	$3p_z$		0.12319	–					
C10	3s	–	0.15098	–					
O11	$2p_x$	–	–	–					
	$2p_y$	–	–	–					
	$2p_z$								
	3s	–	–	–					
	$3p_x$	–	–	–					
	$3p_y$	–	–	–					
	$3p_z$	–	–	–					
C13	3s	–	–	–					
C14	$2p_x$	–	−0.14845	−0.20378					
	$2p_y$	–	−0.13771	0.14109					
	3px	–	−0.22529	−0.23964					
	$3p_y$	–	−0.19226	–					
	$3p_z$	–	0.13901	0.16443					
C15	$2p_x$	–	0.21770	−0.18298					
	$2p_y$	–	0.20064	–					
	$2p_z$	–	−0.16492	0.12975					
	$3p_x$	–	0.29441	−0.23485					
	$3p_z$	–	–	0.17135					
C16	$2p_x$	–	–	−0.10467					
	$3p_x$	–	–	−0.12551					
S20	$2p_y$	–	–	–					
	$3p_x$	–	–	–					
	$3p_z$	–	–	–					

value in the acetamides derivatives of HOMO atomic orbitals while the C3, O5, C7, C9, C10 and N12 atoms have the highest values in the LUMO atomic orbitals.

CONCLUSIONS

The relationship between the quantum chemical parameters and the inhibition efficiency of long alkyl side chain acetamides and isoxazolidine derivatives have been investigated using HF and DFT calculations. The inhibition efficiency of the inhibitor is closely related to the quantum chemical parameters, E_{HOMO}, E_{LUMO}, ΔE, μ, η and ΔN for the neutral inhibitors and no important correlation has been found with parameters for the molecules studies. The compounds studied have been good candidates as second-order nonlinear optical materials because their first hyperpolarizabilities have been changed between 1.26 and 122.44 times that of urea.

REFERENCES

1. Yıldırım, A. and Çetin, M., *Corrosion Sci.*, 2008, vol. 50, p. 155.
2. Ajmal, M., Mideen, A.S., and Quaraishi, M.A., *Corrosion Sci.*, 1994, vol. 36, p. 79.
3. Arslan, T., Kandemirli, F., Ebenso, E.E., et al., *Corrosion Sci.*, 2009, vol. 51, p. 35.
4. Ali, S.A., Saeed, M.T., and Rahman, S.U., *Corrosion Sci.*, 2003, vol. 45, p. 253.
5. Ebenso, E.E., Isabirye, D.A., and Eddy, N.O., *Int. J. Mol. Sci.*, 2010, vol. 11, p. 2473.
6. Ashry, E.S.H.E., Nemr, A.E., Esawy, S.A., and Ragab, S., *Electrochim. Acta*, 2006, vol. 51, p. 3957.
7. Ali, S.A., El-Shareef, A.M., Al-Ghamdi, R.F., and Saeed, M.T., *Corrosion Sci.*, 2005, vol. 47, p. 2659.
8. Wilson, C.O., *J. Am. Pharmaceutical Association,* 1949, vol. 38, p. 466.
9. Craig, B.D. and Anderson, D.S., *Int. Handbook of Corrosion Data*, 2nd ed., 1995, p. 128.
10. Treybig, D.S. and Martinez R.G., Patent US 4957640.
11. Redmore, D. and Outlaw B.T., Patent US 4235838.
12. Ahn, Y.S. and Jovancicevic, V. Patent US 6645399.
13. Kandemirli, F. and Sagdinc, S., *Corrosion Sci.*, 2007, vol. 49, p. 2118.
14. Abraham, J.P., Sajan, D., Hubert, J.I., and Jayakumar, V.S., *Spectrochim. Act*a, Ser. A, 2008, vol. 71, p. 355.
15. Hyper Chem 7.5 Release for Windows, USA, Hypercube Inc., 2003.
16. Frisch, A., Nielsen, A.B., and Holder, A.J., GaussView Users Manual, Pittsburg: Gaussian Inc., 2000.
17. Frisch, M.J., Trucks, G.W., Schlege, H.B., et al., Gaussian 03, Revision B.05, Wallingford: Gaussian Inc., CT, 2004.
18. Parr, R.G., Donnelly, R.A., Levy, M., and Palke, W.E., *J. Chem. Phys.*, 1978, vol. 68, p. 3801.
19. Pearson, R.G., *Inorg Chem.*, 1998, vol. 27, p. 734.
20. Pearson, R.G., *J. Am. Chem. Soc.*, 1963, vol. 85, p. 3533.
21. Pearson, R.G., *Proc. Natl. Acad. Sci. USA*, 1986, vol. 83, p. 8440.
22. Sastri, V.S. and Perumareddi, J.R., *Corrosion*, 1996, vol. 53, p. 671.
23. Martinez, S. and Tagljar, I.S., *J. Mol. Struct. Theochem.*, 2003, vol. 640, p. 167.
24. Avila, G., *J. Chem. Phys.*, 2005, vol. 122, p. 144310.
25. Jeewandara, A.K. and Nalin de Silva, K.M., *J. Mol. Struct. Theochem.*, 2004, vol. 686, p. 131.
26. Ahmed, A.B., Feki, H., Abid, Y., et al., *J. Mol. Struct.*, 2008, vol. 888, p. 180.
27. Ahamad, I., Prasad, R., and Quraishi, M.A., *Corrosion Sci.*, 2010, vol. 52, p. 933.
28. Ebenso, E.E., Arslan, T., Kandemirli, F., et al., *Corrosion Sci.*, 2009, vol. 51, p. 35.
29. Abdallah, M., *Corrosion Sci.*, 2002, vol. 44, p. 717.
30. Hackerman, N. and Hurd, R.M., *Proc. Int. Cong. of Metallic Corrosion*, London: Butterworths, 1962, p. 166.
31. Al, Sk.A., Saeed, M.T., and Rahman, S.U., *Corrosion Sci.*, 2003, vol. 45, p. 253.
32. Hohenberg, P. and Kohn, W., *Inhomogeneous Electron Gas Phys. Rev.*, 1964, vol. 136, p. B864.
33. Sastri, V.S. and Perumareddi, J.R., *Corrosion,* 1997, vol. 53, p. 617.
34. Lukovits, I., Kalman, E., and Zucchi, F., *Corrosion*, 2001, vol. 57, p. 3.
35. Ju, H., Kai, Z.P., and Li, Y., *Corrosion Sci.*, 2008, vol. 50, p. 865.
36. Gece, G., *Corrosion Sci.*, 2008, vol. 50, p. 2981.
37. Zhang, C.R., Chen, H.S., and Wang, G.H., *Chem. Res. Chin.*, 2004, vol. 20, p. 640.
38. Karelson, M. and Lobanov, S., *Chem. Rev.*, 1996, vol. 96, p. 1027.
39. Cheng, H., Feng, J., Ren, A., and Liu, J., *Acta Chim. Sin.*, 2002, vol. 60, p. 830.
40. Cheng, H., Feng, J., and Ren, A., *Acta Chim. Sin.,* 2004, vol. 62, p. 362.
41. Sa, R., Wu, K., Lin, C., et al., *Chin. J. Struct. Chem.,* 2003, vol. 22, p. 481.
42. Cheng, H., Feng, J., Ren, A., and Liu, J., *Acta Chim. Sin.*, 2003, vol. 61, p. 541.
43. Mulliken, R.S., *J. Chem. Phys.*, 1955, vol. 23, p. 1833.
44. Khaled, K.F., *J. Electrochim. Acta*, 2008, vol. 53, p. 3484.
45. Khaled, K.F. and Amin, M.A., *J. Appl. Electrochem.*, 2008, vol. 38, p. 1609.
46. Roque, J.M., Pandiyan, T., Cruz, J., and Gracia-Ochoa, E., *Corrosion Sci.*, 2008, vol. 50, p. 614.
47. Ditchfield, R., Hehre, W.J., and Pople, J.A., *J. Chem. Phys.*, 1971, vol. 54, p. 724.
48. Hehre, W.J., Ditchfield, R., and Pople, J.A., *J. Chem. Phys.*, 1972, vol. 56, p. 2257.
49. Hariharan, P.C. and Pople, J.A., *Mol. Phys.*, 1974, vol. 27, p. 209.
50. Gordon, M.S., *Chem. Phys. Lett.*, 1980, vol. 76, p. 163.
51. Hariharan, P.C. and Pople, J.A., *Theo. Chim. Acta*, 1973, vol. 28, p. 213.
52. Frisch, M.J., Pople, J.A., and Binkley, J.S., *J. Chem. Phys.*, 1984, vol. 80, p. 3265.